

Exploring Soliton Solutions of the Nonlinear Time-Fractional Schrödinger Model via M-Truncated and Atangana-Baleanu Fractional Operators

Fatma Nur Kaya Sağlam¹ 

Article Info

Received: 20 May 2025

Accepted: 21 Jun 2025

Published: 30 Jun 2025

Research Article

Abstract— This study investigates the nonlinear time-fractional Schrödinger model by utilizing this prototype in fields like nonlinear optics, plasma physics, soliton theory, quantum field theory, and dark matter/neural network modeling. It analyzes the equation to reveal key insights into fundamental physical phenomena, advancing novel technological applications. The paper presents fractional derivatives using M-truncated and Atangana-Baleanu operators. The approach employs Bäcklund transformation and Wang's direct mapping method to derive soliton solutions, including exponential, sin-cos, sinh-cosh, rational, trigonometric, and hyperbolic forms. The present study constructs the energy balance method via the problem's Hamiltonian and variational principle, offering a promising approach. It complements analytical results with numerical simulations to enhance understanding of solution behavior. The study provides foundations for further exploration, ensuring practical, reliable solutions for complex nonlinear problems. The methods prove robust, efficient, and applicable to diverse nonlinear PDEs.

Keywords — Bäcklund transformation-based approach, Wang's direct mapping method, energy balance method, soliton solutions

Mathematics Subject Classification (2020) 35A24, 35C08

1. Introduction

Fractional calculus plays a key role by offering a more detailed and accurate mathematical framework for modeling, analyzing, and understanding complex systems and phenomena. It bridges the gap between traditional calculus and the intricate dynamics observed in real-world applications, thereby enabling advancements in technology, scientific research, and various applied fields. Considerable strides have been made in fractional calculus to overcome the limitations of classical differential operators. Consequently, researchers have developed new operators or modified existing ones. The non-singular operator introduced by Caputo and Fabrizio [1] was proposed to resolve the singularity issues present in traditional definitions. However, the Caputo-Fabrizio operator still exhibits non-local behavior, which can be problematic in contexts requiring localized modeling. To simultaneously overcome both singularity and non-locality challenges, Atangana and Baleanu [2] introduced a new fractional operator. This operator forms provides an effective alternative by reducing non-local effects while eliminating singularities.

¹ftmnrtp@gmail.com (Corresponding Author)

¹Department of Mathematics, Faculty of Arts and Sciences, Tekirdağ Namık Kemal University, Tekirdağ, Türkiye

Fractional derivatives have a wide range of implications in various fields, such as physics, transport, fluid motion, elastic media, robotics, mechanics, electromagnetic theory, engineering, geophysics, signal processing, and biology. Recent advancements have shown that fractional derivatives can also be used to describe financial [3] and economic systems [4]. Given that many complex problems can be expressed as fractional differential equations (FDEs), the exploration of both analytical and numerical methods for solving such equations is of significant interest [5,6]. These models are valuable for studying various real-world nonlinear phenomena that arise across diverse disciplines, including engineering, physics, and applied mathematics.

Classical definitions of fractional derivatives often face limitations regarding physical interpretability and are highly sensitive to initial conditions. In contrast, the M-truncated and Atangana–Baleanu (AB) fractional derivatives employed in this study offer significant advantages for modeling complex memory effects and damping behaviors in physical systems. Notably, the Mittag–Leffler kernel associated with the AB derivative enhances its ability to capture long-term effects more accurately than classical approaches. On the other hand, the M-truncated derivative provides greater flexibility in analytical treatment, making it more suitable for various solution strategies. Consequently, both operators serve as effective modeling tools, capable of representing physical processes with both mathematical rigor and practical relevance.

The Schrödinger equation is one of the fundamental models in quantum theory. In the Schrödinger equation, Naber [7] included the time-fractional derivative. This equation is applied in a variety of physics fields, including particle physics, biological systems, nuclear physics, atomic physics, molecular chemistry, astrophysics, solid-state physics, quantum mechanics in nanostructures, condensed matter physics, and quantum information and computing [8].

Several analytical methods have been used to obtain exact soliton solutions. These include the modified generalized Riccati equation mapping method [9], the auxiliary equation method [10], the improved modified Sardar sub-equation method [11], the new version of the generalized exponential rational function method [12], the modified Kudryashov method [13], the sine-cose method [14], the modified extended Tanh expansion method [15], the extended simplest equation method [16], and Lie symmetry analysis and conservation laws [17]. In this study, a nonlinear time-fractional model with M-truncated and AB fractional operators are used. These investigations include both singular and non-singular operators. The Bäcklund transformation-based method, Wang’s direct mapping method, and the energy balance method (EBM) are utilized to obtain the soliton solutions. Additionally, these methods are novel in the literature for the investigated model.

The remaining sections of this paper are organized as follows: Section 2 describes the model used in the study. Section 3 presents the preliminary definitions. Section 4 proposes the fractional model. Section 5 uses the homogeneous balancing approach to obtain the Bäcklund transformation and the ansatz function schemes to construct numerous exact solutions through symbolic computation. Section 6 investigates the various soliton solutions using Wang’s direct mapping method. Section 7 implements the EBM. Section 8 provides comparisons. Section 9 presents the physical properties of the obtained results in graphical form. Finally, Section 10 provides the conclusions.

2. A Summary of the Model

Consider the nonlinear time-fractional Schrödinger equation [18]:

$$iV_t + a_1 V_{xx} + a_2 |V|^2 V = 0 \quad (2.1)$$

where $V = V(x, t)$ represents a complex-valued function depend on both the spatial variable x and the temporal variable t , where $t > 0$. The nonlinear Schrödinger equation is a fundamental equation in quantum mechanics, playing a pivotal role in understanding various phenomena. The model presented is of significant importance in contemporary scientific research and is regarded as a widely applicable indirect model. It arises from diverse applied mathematics and physics areas, including astrophysics, biophysics, plasma dynamics, quantum optics, fluid dynamics, chaos theory, nonlinear wave propagation, and quantum information theory [19]. The specific form considered here is a well-known variant of the classical Schrödinger equation, where the constant parameter a_2 determines the type of soliton solution: a positive a_2 leads to bright solitons, while a negative a_2 produces dark solitons [18]. Previous studies have investigated this model using different fractional derivatives. For example, Gurefe [20] applied Atangana's conformable fractional derivative and obtained five exact solutions via the generalized Kudryashov method. Ahmad et al. [21] used the unified method, and Asjad et al. [22] employed an extended direct algebraic technique to construct multiple exact solutions for the same model.

3. Preliminaries

This section presents the AB fractional operator and the M-truncated operator, along with a description of the operators used.

Definition 3.1. [2] Let $g : [a, b] \rightarrow \mathbb{R}$ be a continuous function and $0 < \varepsilon < 1$. Then, the AB-type fractional operator in the sense of the Riemann–Liouville operator is defined by

$${}_0^{ABR}F_{a+}^{\varepsilon}(g(t)) = \frac{AB(\varepsilon)}{(1-\varepsilon)} \frac{d}{dt} \int_a^t g(t) E_{\varepsilon} \left(\frac{-\varepsilon(t-t)^{\varepsilon}}{1-\varepsilon} \right) dt$$

where the normalization is represented by $AB(\varepsilon)$, and the Mittag-Leffer function is shown by E_{ε} . Consequently,

$${}_0^{ABR}F_{a+}^{\varepsilon}(g(t)) = \frac{AB(\varepsilon)}{(1-\varepsilon)} \sum_{j=0}^{\infty} \left(\frac{-\varepsilon}{1-\varepsilon} \right)^j {}^{RL}I_{\alpha}^{\varepsilon j} g(t)$$

Definition 3.2. [23] Let $h : \mathbb{R}^+ \rightarrow \mathbb{R}$ be a differentiable function, $0 < \varepsilon < 1$, $\gamma > 0$, and $t > 0$. Then, the generalized fractional operator is defined by

$${}_t F_M^{\varepsilon, \gamma}(h(t)) = \lim_{\varepsilon \rightarrow 0} \frac{h(t + {}_t E_{\gamma}(\varepsilon t^{-\varepsilon})) - h(t)}{\varepsilon}$$

in which ${}_t E_{\gamma}(\cdot)$ is a single-parameter Mittag-Leffer function.

Definition 3.3. [24] Let $\gamma > 0$, $Z \in \mathbb{C}$, and $\iota \in \mathbb{N}$. Then, ${}_t E_{\gamma}$ is defined as follows:

$${}_t E_{\gamma}(Z) = \sum_{j=0}^{\iota} \frac{Z^j}{\Gamma(\gamma j + 1)}$$

Theorem 3.4. Let $h : \mathbb{R}^+ \rightarrow \mathbb{R}$ be a function that is continuous at $t = 0$, and differentiable at some $t_0 > 0$ both in the classical and fractional sense of order $\alpha \in (0, 1)$, with a fixed parameter $\gamma > 0$. Then, the function h satisfies the required conditions for the application of the generalized fractional operator.

Theorem 3.5. [23] Let $c_1, c_2, c_3 \in \mathbb{R}$, $0 < \varepsilon \leq 1$, $\gamma > 0$, and $g, h : \mathbb{R}^+ \rightarrow \mathbb{R}$ be differentiable functions for $t > 0$. Then, the following properties hold for the fractional operator ${}_t F_M^{\varepsilon, \gamma}$:

$${}_t F_M^{\varepsilon, \gamma}(c_3) = 0$$

$${}_t F_M^{\varepsilon, \gamma}(k(g(t))) = k({}_t F_M^{\varepsilon, \gamma}(g(t)))$$

$$\begin{aligned} {}_tF_M^{\varepsilon,\gamma}(c_1(g(t)) + c_2(h(t))) &= c_1 {}_tF_M^{\varepsilon,\gamma}(g(t)) + c_2 {}_tF_M^{\varepsilon,\gamma}(h(t)) \\ {}_tF_M^{\varepsilon,\gamma}(h(t) * g(t)) &= (h(t)) {}_tF_M^{\varepsilon,\gamma}(g(t)) * (g(t)) {}_tF_M^{\varepsilon,\gamma}(h(t)) \\ {}_tF_M^{\varepsilon,\gamma}\left(\frac{h(t)}{g(t)}\right) &= \frac{(g(t)) {}_tF_M^{\varepsilon,\gamma}(h(t)) - (h(t)) {}_tF_M^{\varepsilon,\gamma}(g(t))}{(g(t))^2} \\ {}_tF_M^{\varepsilon,\gamma}(t^\vartheta) &= T^{\vartheta-\varepsilon}, \quad \vartheta \in \mathbb{R} \end{aligned}$$

and

$${}_tF_M^{\varepsilon,\gamma}(g(h))(t) = g'(h) {}_tF_M^{\varepsilon,\gamma}(h)$$

4. Fractional Representations of the Aforementioned Model

This section presents the fractional structure of the nonlinear partial differential equation (NLPDE) using two different fractional operators, including both singular and nonsingular kernels.

i. The R-L sense form of (2.1) has the fractional operator AB as

$${}_0^{AB}F_t^\varepsilon V + a_1 V_{xx} + a_2 |V|^2 V = 0$$

where the AB in the context of R-L operators with regard to t is represented by ${}_0^{AB}F_t^\varepsilon$.

ii. The modified M-truncated form of the fractional operator of (2.1) is

$${}_tF_{M,t}^\varepsilon V + a_1 V_{xx} + a_2 |V|^2 V = 0$$

where the modified M-truncated operators based on t is represented by $F_{M,t}^\varepsilon$.

4.1. Construction of the Operational Transformation Scheme

Consider the following wave transformation:

$$V = V(x, t) = L(\xi)e^{i\Theta} \quad (4.1)$$

The analysis of the fractional derivatives will be carried out with respect to ξ and Θ .

i. For the M-truncated operator, we produce ξ and Θ as follows:

$$\xi = x - \frac{2a_4a_5}{\varepsilon} \left(t + \frac{1}{\Gamma(\varepsilon)} \right)^\varepsilon$$

and

$$\Theta = xa_3 + \frac{a_4}{\varepsilon} \left(t + \frac{1}{\Gamma(\varepsilon)} \right)^\varepsilon + \theta \quad (4.2)$$

ii. For the AB operator in RL sense, we produce ξ and Θ as follows:

$$\xi = x - \frac{(1-\varepsilon)(2a_4a_5t^{-n\varepsilon})}{AB(\varepsilon) \sum_{n=0}^{\infty} \left(\frac{-\varepsilon}{1-\varepsilon} \right) \Gamma(1-\varepsilon n)}$$

and

$$\Theta = a_3x + \frac{(1-\varepsilon)(a_4t^{-n\varepsilon})}{AB(\varepsilon) \sum_{n=0}^{\infty} \left(\frac{-\varepsilon}{1-\varepsilon} \right) \Gamma(1-\varepsilon n)} + \theta \quad (4.3)$$

5. Methodology

Consider the subsequent NLPDE:

$$P_1(V, V_x, V_t, V_{xx}, V_{xt}, \dots) = 0 \quad (5.1)$$

in which (5.1) is satisfied by $V = V(x, t)$. By applying the transformation given in (4.1), where ξ is defined accordingly, the formulation is considered both for the M-truncated operator as in (4.2) and for the AB operator in the Riemann–Liouville sense as in (4.3). Consequently, (5.1) is transformed into an nonlinear ordinary differential equation (NODE) as follows:

$$P_2(L, L', L'', \dots) = 0 \quad (5.2)$$

Applying (4.1) into (2.1), the imaginary and real components are obtained as follows, respectively:

$$a_5 = \frac{a_1 a_3}{a_4}$$

and

$$a_1 L'' - (a_4 + a_1 a_3^2) L + a_2 L^3 = 0 \quad (5.3)$$

5.1. Bäcklund Transformation and Implementing

Assume that (5.2) provides the subsequent solution form [25]:

$$L = A_1 \frac{\partial^\varrho \hbar}{\partial \xi^\varrho} + A_2 \quad (5.4)$$

To calculate the value of the equilibrium parameter ϱ , we utilize (5.3) to balance L'' and L^3 . Thus, $\varrho = 1$.

5.1.1. Type-I: Exponential Function

Assume that

$$\hbar(\xi) = \ln(n_1 \exp(-\xi) + n_0 + n_2 \exp(\xi)) \quad (5.5)$$

where n_i such that $i \in \{0, 1, 2\}$ are real parameters. By putting (5.4) with (5.5) into (5.3) and taking the coefficients of $\exp(\xi)$ as zero, an algebraic equation system is produced. The solutions of this system are obtained as follows:

Set I.

$$n_0 = n_0, \quad n_1 = 0, \quad n_2 = n_2, \quad a_1 = -\frac{2a_4}{2a_3^2 + 1}, \quad A_1 = -\sqrt{\frac{4a_4}{(2a_2a_3^2 + a_2)}}, \quad \text{and} \quad A_2 = \sqrt{\frac{a_4}{(2a_2a_3^2 + a_2)}}$$

Combining (5.4), (5.5), and (4.1) with above results, the exponential function solution of (2.1) is obtained as follows:

$$V_{1,1,1}(x, t) = -\frac{\sqrt{\frac{a_4}{2a_3^2 + 1}} (n_2 \exp(\xi) - n_0)}{n_0 + n_2 \exp(\xi)} e^{i(\Theta)} \quad (5.6)$$

Here, ξ and Θ are expressed in (4.2) for the M-truncated operator form and in (4.3) for the AB operator form in RL sense, respectively.

Set II.

$$n_0 = n_0, \quad n_1 = n_1, \quad n_2 = 0, \quad a_1 = -\frac{2a_4}{2a_3^2 + 1}, \quad A_1 = \sqrt{\frac{4a_4}{(2a_2a_3^2 + a_2)}}, \quad \text{and} \quad A_2 = \sqrt{\frac{a_4}{(2a_2a_3^2 + a_2)}}$$

Combining (5.4), (5.5), and (4.1) with above results, the exponential function solution of (2.1) is obtained as follows:

$$V_{1,1,2}(x, t) = -\frac{\sqrt{\frac{a_4}{a_2(2a_3^2+1)}} (n_1 \exp(-\xi) - n_0)}{n_0 + n_1 \exp(-\xi)} e^{i(\Theta)}$$

Here, ξ and Θ are expressed in (4.2) for the M-truncated operator form and in (4.3) for the AB operator form in RL sense, respectively.

Set III.

$$n_0 = 2\sqrt{n_1 n_2}, \quad n_1 = n_1, \quad n_2 = n_2, \quad a_1 = -\frac{2a_4}{2a_3^2 + 1}, \quad A_1 = \sqrt{\frac{a_4}{(2a_2 a_3^2 + a_2)}}, \quad \text{and} \quad A_2 = 0$$

Combining (5.4), (5.5), and (4.1) with above results, the exponential function solution of (2.1) is obtained as follows:

$$V_{1,1,3}(x, t) = -\frac{\sqrt{\frac{a_4}{a_2(2a_3^2+1)}} (n_1 \exp(-\xi) - n_2 \exp(\xi))}{n_1 \exp(-\xi) + 2\sqrt{n_1 n_2} + n_2 \exp(\xi)} e^{i(\Theta)}$$

Here, ξ and Θ are expressed in (4.2) for the M-truncated operator form and in (4.3) for the AB operator form in RL sense, respectively.

Set IV.

$$n_0 = 0, \quad n_1 = n_1, \quad n_2 = n_2, \quad a_1 = -\frac{a_4}{a_3^2 + 2}, \quad A_1 = \sqrt{\frac{4a_4}{(2a_2 a_3^2 + a_2)}}, \quad \text{and} \quad A_2 = 0$$

Combining (5.4), (5.5), and (4.1) with above results, the exponential function solution of (2.1) is obtained as follows:

$$V_{1,1,4}(x, t) = -\frac{\sqrt{\frac{4a_4}{a_2(2a_3^2+1)}} (n_1 \exp(-\xi) - n_2 \exp(\xi))}{n_1 \exp(-\xi) + n_2 \exp(\xi)} e^{i(\Theta)}$$

Here, ξ and Θ are expressed in (4.2) for the M-truncated operator form and in (4.3) for the AB operator form in RL sense, respectively.

5.1.2. Type-II: Sin-Cos Function

Assume that

$$\hbar(\xi) = \ln(n_0 \cos(\xi) + n_1 + n_2 \sin(\xi)) \quad (5.7)$$

where n_i such that $i \in \{0, 1, 2\}$ are real parameters. By putting (5.4) with (5.7) into (5.3) and taking the coefficients of $\cos(\xi)$ and $\sin(\xi)$ as zero, an algebraic equation system is produced. The solution of this system is reached as follows:

Set I.

$$n_0 = n_0, \quad n_1 = n_1, \quad n_2 = -\frac{a_2 n_0 (2a_3^2 - 1)}{a_4} \sqrt{-\frac{a_4}{(2a_2 a_3^2 - a_2)}} \sqrt{\frac{a_4}{(2a_2 a_3^2 - a_2)}}, \quad a_1 = -\frac{2a_4}{2a_3^2 - 1}$$

$$A_1 = \sqrt{\frac{4a_4}{(2a_2 a_3^2 - a_2)}}, \quad \text{and} \quad A_2 = \sqrt{-\frac{a_4}{(2a_2 a_3^2 - a_2)}}$$

Combining (5.4), (5.7), and (4.1) with above results, the sin-cos function solution of (2.1) is obtained

as follows:

$$V_{2,1,1}(x, t) = \frac{a_4 \begin{pmatrix} \sin(\xi) n_0 \sqrt{\frac{a_4}{a_2(2a_3^2-1)}} \\ + \cos(\xi) n_0 \sqrt{-\frac{a_4}{a_2(2a_3^2-1)}} \\ - \sqrt{-\frac{a_4}{a_2(2a_3^2-1)}} n_1 \end{pmatrix}}{\begin{pmatrix} (2 \sin(\xi) a_2 a_3^2 n_0 - \sin(\xi) a_2 n_0) \sqrt{\frac{a_4}{a_2(2a_3^2-1)}} \sqrt{-\frac{a_4}{a_2(2a_3^2-1)}} \\ - \cos(\xi) a_4 n_0 - a_4 n_1 \end{pmatrix}} e^{i(\Theta)} \quad (5.8)$$

Here, ξ and Θ are expressed in (4.2) for the M-truncated operator form and in (4.3) for the AB operator form in RL sense, respectively.

5.1.3. Type-III: Sinh–Cosh Function

Assume that

$$\hbar(\xi) = \ln(n_0 \cosh(\xi) + n_1 + n_2 \sinh(\xi)) \quad (5.9)$$

where n_i such that $i \in \{0, 1, 2\}$ are real parameters. By putting (5.4) with (5.9) into (5.3) and taking the coefficients of $\cos(\xi)$ and $\sin(\xi)$ as zero, an algebraic equation system is produced. The solution of this system is attained as follows:

Set I.

$$n_0 = n_0, \quad n_1 = n_1, \quad n_2 = -\frac{a_2 n_0 (2a_3^2 + 1)}{(2a_2 a_3^2 + a_2)}, \quad a_1 = -\frac{2a_4}{2a_3^2 + 1},$$

$$A_1 = \sqrt{\frac{4a_4}{(2a_2 a_3^2 + a_2)}}, \quad \text{and} \quad A_2 = \sqrt{\frac{a_4}{(2a_2 a_3^2 + a_2)}}$$

Combining (5.4), (5.9), and (4.1) with above results, the sinh–cosh function solution of (2.1) is obtained as follows:

$$V_{3,1,1}(x, t) = -\frac{\sqrt{\frac{a_4}{a_2(2a_3^2+1)}} (\sinh(\xi) n_0 - \cosh(\xi) n_0 + n_1)}{(\sinh(\xi) n_0 - \cosh(\xi) n_0 - n_1)} e^{i(\Theta)}$$

Here, ξ and Θ are expressed in (4.2) for the M-truncated operator form and in (4.3) for the AB operator form in RL sense, respectively.

5.1.4. Type-IV: Rational Function

Assume that

$$\hbar(\xi) = \ln(n_0 + n_1(\xi)) \quad (5.10)$$

where n_i such that $i \in \{0, 1, 2\}$ are real parameters. By putting (5.4) with (5.10) into (5.3) and taking the coefficients of $\cos(\xi)$ and $\sin(\xi)$ as zero, an algebraic equation system is produced. The solution of this system is gained as follows:

Set I.

$$n_0 = n_0, \quad n_1 = n_1, \quad n_2 = n_2, \quad a_1 = -\frac{a_4}{a_3^2}, \quad A_1 = \frac{\sqrt{\frac{2a_4}{a_2}}}{a_3}, \quad \text{and} \quad A_2 = 0$$

Combining (5.4), (5.10), and (4.1) with above results, the rational function solution of (2.1) is obtained as follows:

$$V_{4,1,1}(x, t) = -\frac{\sqrt{\frac{a_4}{a_2(2a_3^2+1)}} (\sinh(\xi) n_0 - \cosh(\xi) n_0 + n_1)}{(\sinh(\xi) n_0 - \cosh(\xi) n_0 - n_1)} e^{i(\Theta)}$$

Here, ξ and Θ are expressed in (4.2) for the M -truncated operator form and in (4.3) for the AB operator form in RL sense, respectively.

6. Wang's Direct Mapping Approach

In this section, (5.3) is addressed using Wang's direct mapping approach. This approach gives the auxiliary function listed below [25]:

$$\left(\Lambda'(\xi)\right)^2 = \varphi \tau^2 \Lambda^2(\xi) + \frac{\vartheta \tau^2}{\rho^2} \Lambda^4(\xi)$$

where

$$\Lambda(\xi) = \rho \sec h(\tau \xi), \quad \varphi = 1 \text{ and } \vartheta = -1$$

$$\Lambda(\xi) = \rho \csc h(\tau \xi), \quad \varphi = 1 \text{ and } \vartheta = 1$$

$$\Lambda(\xi) = \rho \sec(\tau \xi), \quad \varphi = -1 \text{ and } \vartheta = 1$$

and

$$\Lambda(\xi) = \rho \csc(\tau \xi), \quad \varphi = -1 \text{ and } \vartheta = 1 \quad (6.1)$$

If (5.3) is integrated with respect to ξ and the integral constant is set to zero, the following results are obtained:

$$\left(L'\right)^2 = -\frac{a_2}{2a_1} L^4 + \frac{(a_1 a_3^2 + a_4)}{a_1} L^2 \quad (6.2)$$

Using (6.2) to map (6.1), the solution are derived as follows:

Set I.

$$\varphi = 1, \quad \vartheta = -1, \quad \tau^2 = \frac{a_1 a_3^2 + a_4}{a_1}, \quad \frac{\tau^2}{\rho^2} = \frac{a_2}{2a_1}, \quad \tau = \frac{\sqrt{a_1(a_1 a_3^2 + a_4)}}{a_1}, \quad \text{and} \quad \rho = \frac{\sqrt{2a_2(a_1 a_3^2 + a_4)}}{a_1}$$

Applying the method's steps together with the above results, the solution to (2.1) is obtained as follows:

$$V_{2,2,1}(x, t) = \frac{\sqrt{2a_2(a_1 a_3^2 + a_4)} \sec h\left(\frac{\sqrt{a_1(a_1 a_3^2 + a_4)}}{a_1} \xi\right)}{a_2} e^{i(\Theta)} \quad (6.3)$$

Set II.

$$\varphi = 1, \quad \vartheta = 1, \quad \tau^2 = \frac{a_1 a_3^2 + a_4}{a_1}, \quad \frac{\tau^2}{\rho^2} = -\frac{a_2}{2a_1}, \quad \tau = \frac{\sqrt{a_1(a_1 a_3^2 + a_4)}}{a_1}, \quad \text{and} \quad \rho = \frac{\sqrt{-2a_2(a_1 a_3^2 + a_4)}}{a_1}$$

Applying the method's steps together with the above results, the solution to (2.1) is obtained as follows:

$$V_{2,2,2}(x, t) = \frac{\sqrt{-2a_2(a_1 a_3^2 + a_4)} \csc h\left(\frac{\sqrt{a_1(a_1 a_3^2 + a_4)}}{a_1} \xi\right)}{a_2} e^{i(\Theta)}$$

Set III.

$$\varphi = 1, \quad \vartheta = -1, \quad \tau^2 = \frac{a_1 a_3^2 + a_4}{a_1}, \quad \frac{\tau^2}{\rho^2} = \frac{a_2}{2a_1}, \quad \tau = \frac{\sqrt{a_1(a_1 a_3^2 + a_4)}}{a_1}, \quad \text{and} \quad \rho = \frac{\sqrt{2a_2(a_1 a_3^2 + a_4)}}{a_1}$$

Applying the method's steps together with the above results, the solution to (2.1) is obtained as follows:

$$V_{2,2,3}(x, t) = \frac{\sqrt{2a_2(a_1 a_3^2 + a_4)} \sec\left(\frac{\sqrt{a_1(a_1 a_3^2 + a_4)}}{a_1} \xi\right)}{a_2} e^{i(\Theta)}$$

Set IV.

$$\varphi = 1, \quad \vartheta = -1, \quad \tau^2 = \frac{a_1 a_3^2 + a_4}{a_1}, \quad \frac{\tau^2}{\rho^2} = \frac{a_2}{2a_1}, \quad \tau = \frac{\sqrt{a_1 (a_1 a_3^2 + a_4)}}{a_1}, \quad \text{and} \quad \rho = \frac{\sqrt{2a_2 (a_1 a_3^2 + a_4)}}{a_1}$$

Applying the method's steps together with the above results, the solution to (2.1) is obtained as follows:

$$V_{2,2,4}(x, t) = \frac{\sqrt{2a_2 (a_1 a_3^2 + a_4)} \csc \left(\frac{\sqrt{a_1 (a_1 a_3^2 + a_4)}}{a_1} \xi \right)}{a_2} e^{i(\Theta)}$$

7. EBM

To apply the EBM, we refer to (5.3), as presented in [26]:

$$L'' - \frac{(a_4 + a_1 a_3^2)}{a_1} L + \frac{a_2}{a_1} L^3 = 0 \quad (7.1)$$

The subsequent is the expression for the relevant variational principle:

$$Y(L) = \int_0^{\frac{\pi}{4}} \left(\frac{1}{2} L' + \frac{(a_4 + a_1 a_3^2)}{2a_1} L^2 - \frac{a_2}{4a_1} L^4 \right) d\xi$$

This implies that

$$Y(L) = \int_0^{\frac{\pi}{4}} \left(\frac{1}{2} L' - \left[\frac{a_2}{4a_1} L^4 - \frac{(a_4 + a_1 a_3^2)}{2a_1} L^2 \right] \right) d\xi = \int_0^{\frac{\pi}{4}} (R - P) d\xi$$

Here, R and P represents kinetic energy and potential energy and are expressed as follows, respectively:

$$R = \frac{1}{2} L' \quad \text{and} \quad P = \frac{a_2}{4a_1} L^4 - \frac{(a_4 + a_1 a_3^2)}{2a_1} L^2$$

Therefore, the Hamiltonian invariant is given by

$$H = R + P = \frac{1}{2} L' + \frac{a_2}{4a_1} L^4 - \frac{(a_4 + a_1 a_3^2)}{2a_1} L^2$$

The solution to (7.1) can be written as follows:

$$L(\xi) = K \cos(\varphi \xi) \quad (7.2)$$

Based on the EBM, the Hamiltonian invariant must remain constant, i.e.,

$$H = P + R = \frac{1}{2} L' + \frac{a_2}{4a_1} L^4 - \frac{(a_4 + a_1 a_3^2)}{2a_1} L^2 = H_0 \quad (7.3)$$

For (7.2), the initial conditions are expressed as:

$$L'(0) = 0 \quad \text{and} \quad L(0) = K$$

By replacing these into (7.3),

$$L_0 = \frac{a_2}{4a_1} K^4 - \frac{(a_4 + a_1 a_3^2)}{2a_1} K^2 \quad (7.4)$$

Inserting the expressions from (7.4) and (7.2) into (7.3) leads to the following equality:

$$\frac{1}{2} (-\zeta K \cos(\zeta \xi))^2 + \frac{a_2}{4a_1} (K \cos(\zeta \xi))^4 - \frac{(a_4 + a_1 a_3^2)}{2a_1} (K \cos(\zeta \xi))^2 = \frac{a_2}{4a_1} K^4 - \frac{(a_4 + a_1 a_3^2)}{2a_1} K^2 \quad (7.5)$$

After applying $\zeta \xi = \frac{\pi}{4}$ to (7.5),

$$\frac{1}{4} \zeta^2 K^2 + \frac{a_2}{16a_1} K^4 - \frac{(a_4 + a_1 a_3^2)}{4a_1} K^2 = \frac{a_2}{4a_1} K^4 - \frac{(a_4 + a_1 a_3^2)}{2a_1} K^2$$

Consequently,

$$\zeta = \frac{\sqrt{a_1 (3K^2 a_2 - 4a_1 a_3^2 - 4a_4)}}{2a_1}$$

Therefore, the following statement is the outcomes to (5.2):

$$L(x, t) = K \cos(\zeta \xi)$$

After entering L 's value into (5.1),

$$V_{3,1,1}(x, t) = K \cos(\zeta \xi) e^{i(\Theta)} \quad (7.6)$$

8. Comparisons

In this paper, the Bäcklund transformation-based method, Wang's direct mapping methodology, and the EBM have been used to generate new soliton solutions for the mathematical and physical problems describing by nonlinear fractional model. Gurefe [20] analyzed the model using Atangana's conformable fractional derivative. He produced only five results using the generalized Kudryashov technique. Ahmad et al. [21] applied the unified technique. Asjad et al. [22] used the novel extended direct algebraic technique to obtain several solutions for the model. Notably, the current study has yielded new solutions with various physical properties, such as bright solitons and periodic-type wave structures. The soliton solutions have a wide range of critical real-world applications in fields such as nonlinear optics, phase evolution, chaos theory, condensed matter physics, astronomy, fluid mechanics, biology, and nonlinear quantum field theory. The obtained solutions provide valuable insights into the physical behaviors of the modal. Moreover, a visual depiction of the solutions, systematically derived through analytical methods, is included.

9. Physical Interpretation

This section provides a graphical interpretation of some of the solutions derived from the nonlinear fractional model. Various soliton solutions of the prototype were constructed using the Bäcklund transformation-based method, Wang's direct mapping approach, and EBM.

In Figures 1 and 2, the periodic waves behavior are investigated using M-truncated operators in subfigures a, b, and c and AB fractional operators in subfigures d, e, and f. In Figures 3 and 4, the dark-bright soliton behavior are investigated using M-truncated operators in subfigures a, b, and c and AB fractional operators in subfigures d, e, and f. In Figure 1, the 3d, 2d, and contour plots for the real part of $V_{1,1,1}(x, t)$ in (5.6) with fractional order $\varepsilon = 0.5$, by choosing the values $a_4 = 3$, $a_2 = 2$, $a_3 = 1$, $n_0 = 1.5$, $n_2 = 7$, $a_1 = 0.7$, $n = 0.5$, and $\theta = 0$. In Figure 2, the 3d, 2d, and contour plots for the real part of $V_{2,1,1}(x, t)$ in (5.8) with fractional order $\varepsilon = 0.5$, by choosing the values $a_4 = 1.7$, $a_2 = 0.9$, $a_3 = 0.2$, $n_0 = 1$, $n_1 = 2$, $a_1 = 0.4$, $n = 1$, and $\theta = 0$. In Figure 3, the 3d, 2d, and contour plots for the real part of $V_{2,2,1}(x, t)$ in (6.3) with fractional order $\varepsilon = 0.5$, by choosing the values $a_4 = 0.7$, $a_2 = 1.2$, $a_3 = 0.5$, $a_1 = 0.07$, $n = 0.5$, and $\theta = 0$. In Figure 4, the 3d, 2d, and contour plots for the real part of $V_{3,1,1}(x, t)$ in (7.6) with fractional order $\varepsilon = 0.5$, by choosing the values $a_4 = 0.02$, $a_2 = 4$, $a_3 = 0.5$, $a_1 = 1.9$, $K = 1$, $n = 0.5$, and $\theta = 0$.

The parameters in the diagrams have distinct physical meanings. Whereas a_2 describes the type and degree of nonlinearity in the system, a_1 is the dispersion coefficient that controls the wave spreading behavior throughout space. Whether a solution covers a bright or dark soliton depends on the sign of a_2 . Whereas a_4 aids in the temporal phase evolution, a_3 influences the spatial phase modulation. The memory effect in the system is controlled by the parameter ε , which represents the order of

the fractional derivative. Stronger nonlocal temporal effects are associated with lower levels of ε . Together, these parameters determine the outcome of soliton structures' propagation, shape, and stability properties.

In particular, the effect of the fractional order ε changes depending on whether the M-truncated or AB fractional operators are used. By changing the fractional order ε , the impact of previous states on the system's current behavior is directly changed. In the AB operator situation, the dispersive smoothing in the wave propagation is improved by decreasing ε because it increases the nonlocal interactions caused by the Mittag-Leffler kernel. Energy spreads throughout a greater area, making solutions smoother and broader. In contrast, because the influence range is bounded and the kernel is truncated for the M-truncated operator, the fractional order has a more localized mathematical effect. Sharp, high-amplitude solitons can appear for small ε because of increased nonlinearity and limited dispersion, but solutions shift to more classical waveforms as ε grows. This shows that the two operators are not affected by the same fractional order ε in the same way; the M-truncated derivative shows more sensitive and localized alterations, whilst the AB derivative reacts more slowly and universally.

By assigning specific values to the parameters, periodic waves and dark-bright soliton solutions were obtained from these results. Periodic solitons are wave structures that continuously repeat in a specific pattern and are often observed in media, such as optical fibers, water waves, or plasma. They enable the undistorted and stable propagation of energy-carrying waves through a medium. Dark-bright solitons combine structures in which the intensity decreases in one part of a wave packet dark soliton, and increases in the other part, a bright soliton. Such solutions have critical applications, particularly in optical systems and atomic physics, because combining two opposite interactions offers opportunities for innovative applications in areas such as energy and information transport, lasers, or quantum computing. These solutions are fundamental tools for understanding and controlling physical processes described by nonlinear equations. It is important to emphasize that the findings and solutions presented in this paper are novel and have not been previously documented.

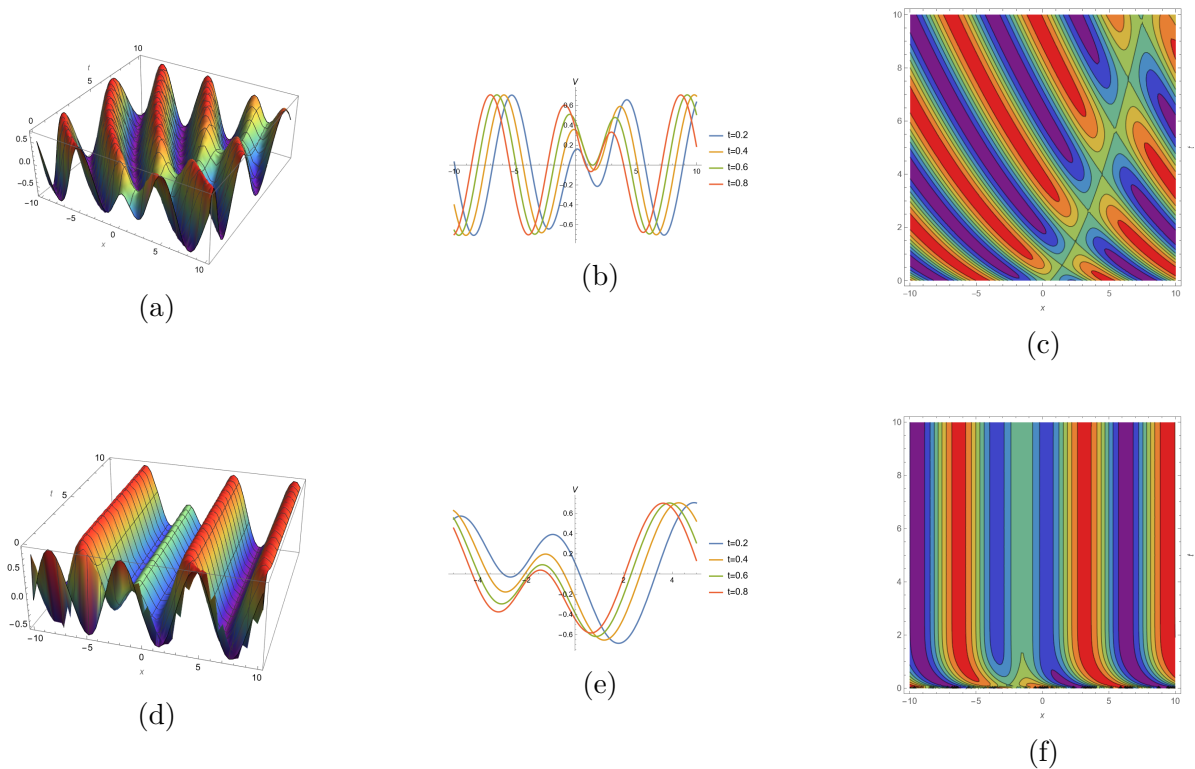


Figure 1. Effects of (a)-(c) the M-truncated and (d)-(f) AB fractional operators of $V_{1,1,1}(x, t)$

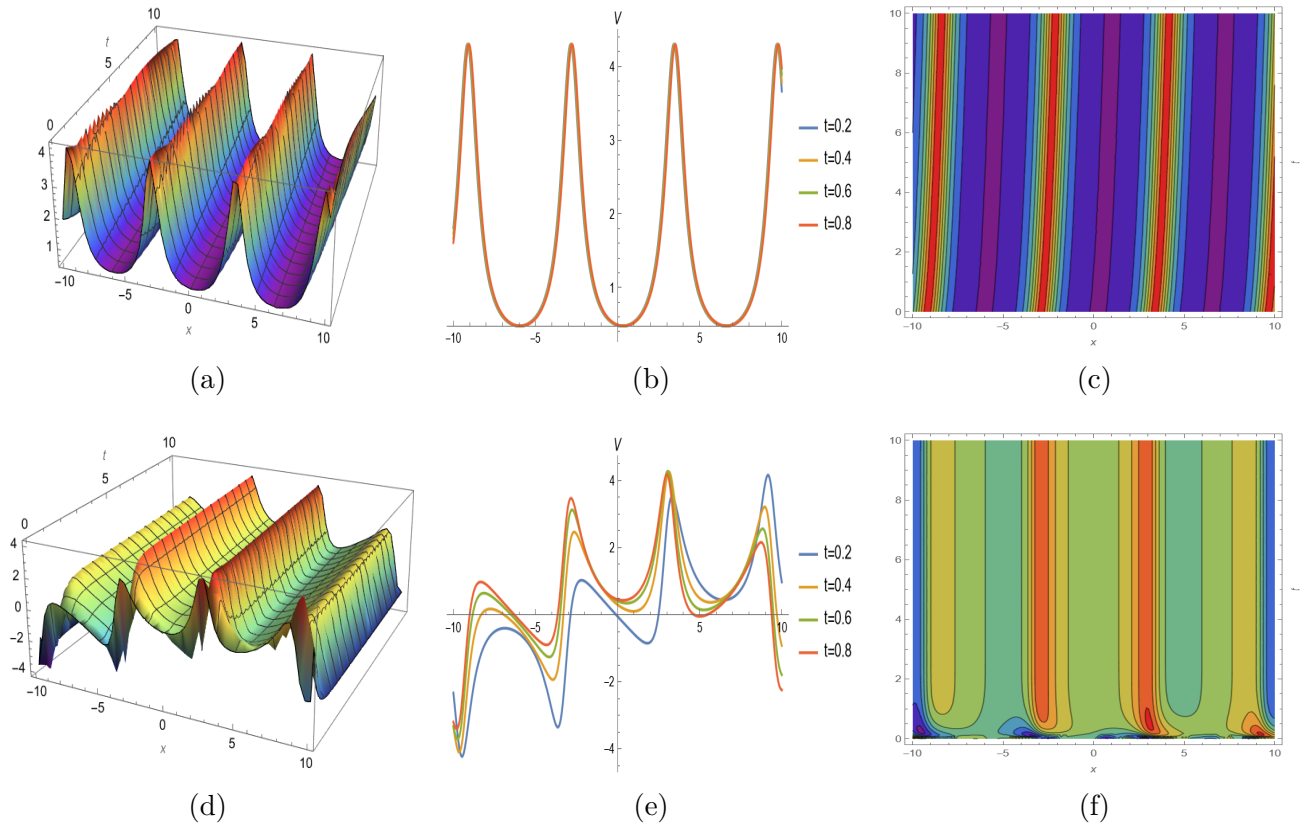


Figure 2. Effects of (a)-(c) the M-truncated and (d)-(f) AB fractional operators of $V_{2,1,1}(x, t)$

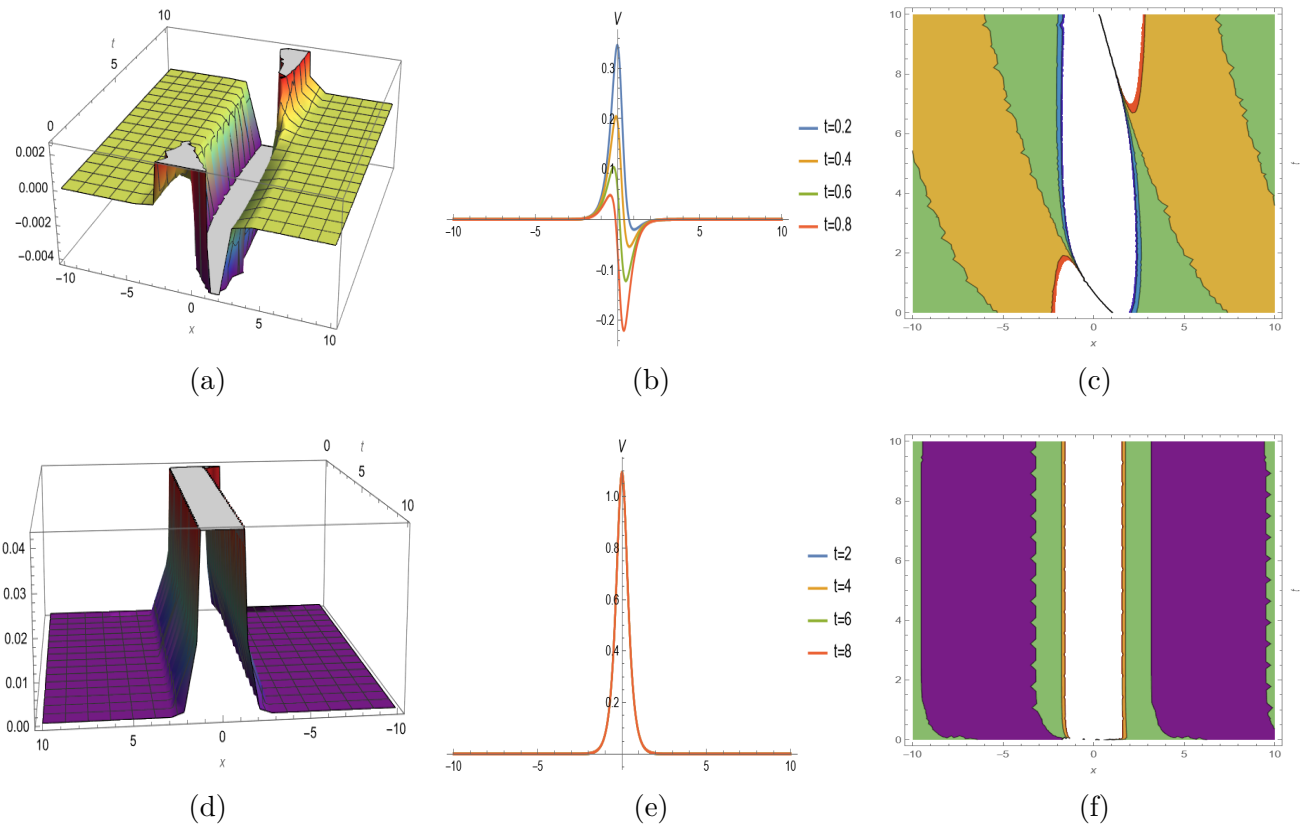


Figure 3. Effects of (a)-(c) the M-truncated and (d)-(f) AB fractional operators of $V_{2,2,1}(x, t)$

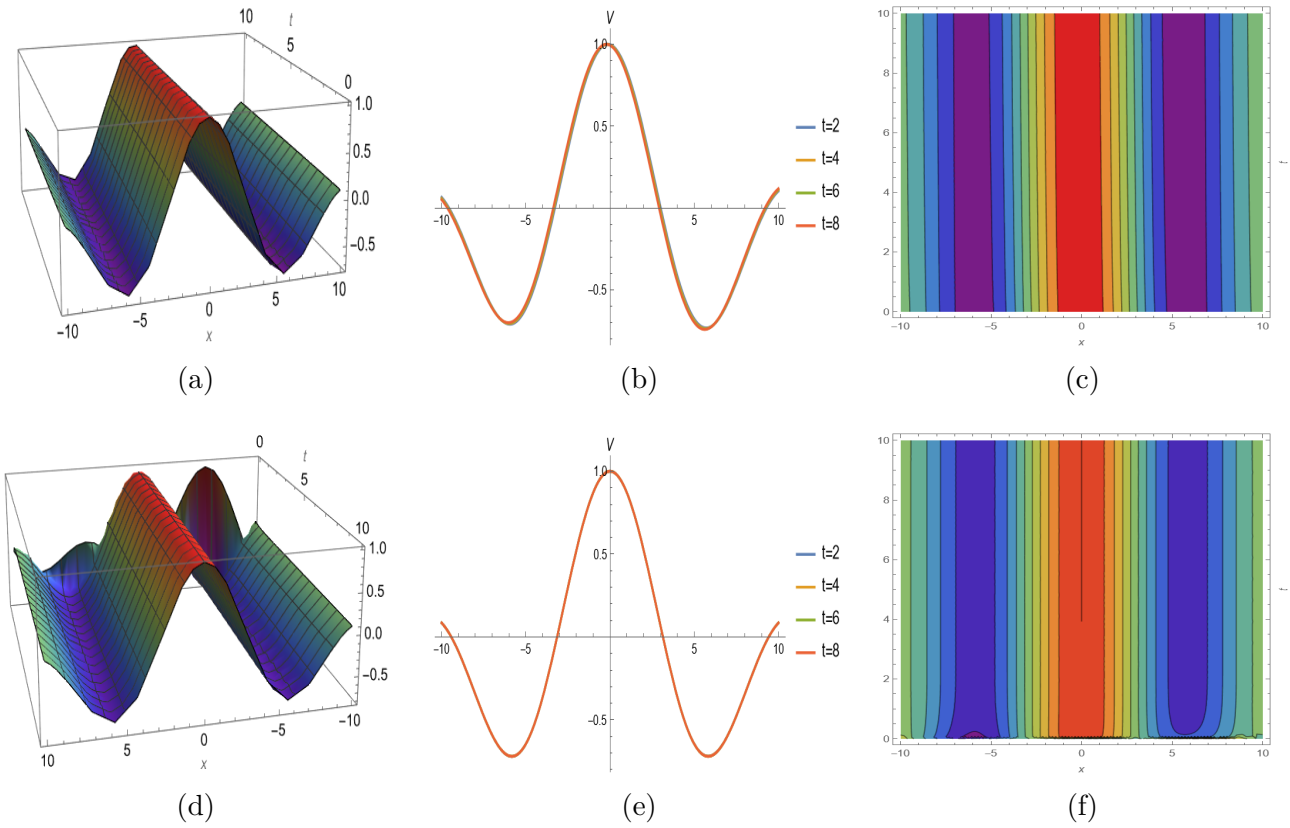


Figure 4. Effects of (a)-(c) the M-truncated and (d)-(f) AB fractional operators of $V_{3,1,1}(x, t)$

10. Conclusion

This study investigated the nonlinear time-fractional Schrödinger model's wave propagation, which arises in different fields of physics and mathematics. Fractional transformations for the wave variables ξ and θ using M-truncated and AB fractional operators were applied to the prototype and converted to a nonlinear ordinary differential equation. Two new approaches, the Bäcklund transformation-based method and Wang's direct mapping method, were used to find a wide range of optical soliton solutions. The solutions for a wide range of solitons were obtained by expressing them as exponential wave solutions, sin-cos wave solutions, sinh-cosh wave solutions, rational wave solutions, trigonometric functions, and hyperbolic function solutions. The EBM was also used, providing an efficient approach by deriving the Hamiltonian and applying the variational principle to the problem. In addition, 3d, 2d, and contour plots were used to illustrate the profiles of different soliton solutions. The findings obtained by the investigated techniques demonstrate that these techniques effectively examine nonlinear wave equations, enhancing the comprehension of their complicated structures and expanding the potential for theoretical investigation. The applied methods are adaptable and applicable to many different types of NLPDEs. Although the methods are pretty flexible, they can not be suitable for all NLPDEs, particularly those that do not satisfy the predetermined criteria or structures that these methods can handle. Future research could concentrate on analyzing these solutions' behavior under various circumstances and investigating their physical effects. This will help to improve science in physics and its broader applications while offering a greater knowledge of nonlinear wave processes.

Author Contributions

The author read and approved the final version of the paper.

Conflicts of Interest

The author declares no conflict of interest.

Ethical Review and Approval

No approval from the Board of Ethics is required.

References

- [1] M. Caputo, M. Fabrizio, *A new definition of fractional derivative without singular kernel*, Progress in Fractional Differentiation & Applications 1 (2) (2015) 73–85.
- [2] A. Atangana, D. Baleanu, *New fractional derivatives with nonlocal and non-singular kernel: Theory and application to heat transfer model*, Thermal Science 20 (2) (2016) 763–769.
- [3] F. Mainardi, M. Raberto, R. Gorenflo, E. Scalas, *Fractional calculus and continuous-time finance II: The waiting-time distribution*, Physica A: Statistical Mechanics and its Applications 287 (3-4) (2000) 468–481.
- [4] N. Laskin, *Fractional market dynamics*, Physica A: Statistical Mechanics and its Applications 287 (3-4) (2000) 482–492.
- [5] A. Ercan, *Fractional kinetic models for drying using a semi-empirical method in the framework of different types of kernels* Symmetry 17 (4) (2025) 483.
- [6] A. Ercan, *Comparative analysis for fractional nonlinear Sturm-Liouville equations with singular and non-singular kernels* AIMS Mathematics 7 (7) (2022) 13325–13343.
- [7] M. Naber, *Time fractional Schrödinger equation*, Journal of Mathematical Physics 45 (8) (2004) 3339–3352.
- [8] N. A. Khan, T. Hameed, *An implementation of Haar wavelet based method for numerical treatment of time-fractional Schrödinger and coupled Schrödinger systems*, IEEE/CAA Journal of Automatica Sinica 6 (1) (2019) 177–187.
- [9] I. S. Hamad, K. K. Ali, *Investigation of Brownian motion in stochastic Schrödinger wave equation using the modified generalized Riccati equation mapping method*, Optical and Quantum Electronics 56 (6) (2024) 1–23.
- [10] Y. Du, T. Yin, J. Pang, *The exact solutions of Schrödinger–Hirota equation based on the auxiliary equation method*, Optical and Quantum Electronics 56 (5) (2024) 712.
- [11] M. I. Khan, A. Farooq, K. S. Nisar, N. A. Shah, *Unveiling new exact solutions of the unstable nonlinear Schrödinger equation using the improved modified Sardar sub-equation method*, Results in Physics 59 (2024) 107593.
- [12] B. Kopçasız, *Qualitative analysis and optical soliton solutions galore: Scrutinizing the (2+1)-dimensional complex modified Korteweg–de Vries system*, Nonlinear Dynamics 112 (23) (2024) 21321–21341.
- [13] M. Mirzazadeh, L. Akinyemi, M. Şenol, K. Hosseini, *A variety of solitons to the sixth-order dispersive (3+1)-dimensional nonlinear time-fractional Schrödinger equation with cubic-quintic-septic nonlinearities*, Optik 241 (2021) 166318.

- [14] V. Ala, G. Shaikhova, *Analytical solutions of nonlinear Beta fractional Schrödinger equation via Sine-Cosine method*, Lobachevskii Journal of Mathematics 43 (11) (2022) 3033–3038.
- [15] F. N. Kaya Sağlam *New analytical wave structures for the $(2+1)$ -dimensional Chaffee-Infante equation*, Universal Journal of Mathematics and Applications 8 (1) (2025) 41–55.
- [16] H. U. Rehman, G. S. Said, A. Amer, H. Ashraf, M. M. Tharwat, M. Abdel-Aty, M. S. Osman, *Unraveling the $(4+1)$ -dimensional Davey-Stewartson-Kadomtsev-Petviashvili equation: Exploring soliton solutions via multiple techniques*, Alexandria Engineering Journal 90 (2024) 17–23.
- [17] B. Kopçasız, E. Yaşar, *Dual-mode nonlinear Schrödinger equation (DMNLSE): Lie group analysis, group invariant solutions, and conservation laws*, International Journal of Modern Physics B 38 (02) (2024) 2450020.
- [18] M. J. Ablowitz, *Nonlinear dispersive waves: Asymptotic analysis and solitons*, Cambridge University Press, 2011.
- [19] V. N. Serkin, A. Hasegawa, *Novel soliton solutions of the nonlinear Schrödinger equation model*, Physical Review Letters 85 (21) (2000) 4502.
- [20] Y. Gurefe, *The generalized Kudryashov method for the nonlinear fractional partial differential equations with the beta-derivative*, Revista Mexicana de Física 66 (6) (2020) 771–781.
- [21] H. Ahmad, M. N. Alam, M. A. Rahim, M. F. Alotaibi, M. Omri, *The unified technique for the nonlinear time-fractional model with the beta-derivative*, Results in Physics 29 (2021) 104785.
- [22] M. I. Asjad, M. Inc, W. A. Faridi, M. A. Bakar, T. Muhammad, H. Rezazadeh, *Optical solitonic structures with singular and non-singular kernel for nonlinear fractional model in quantum mechanics*, Optical and Quantum Electronics 55 (3) (2023) 219.
- [23] J. V. da C. Sousa, E. C. de Oliveira, *A new truncated M -fractional derivative type unifying some fractional derivative types with classical properties*, International Journal of Analysis and Applications 16 (1) (2018) 83–96.
- [24] W. Liu, K. Chen, *The functional variable method for finding exact solutions of some nonlinear time-fractional differential equations*, Pramana 81 (2013) 377–384.
- [25] M. Wang, Y. Wang, *A new Bäcklund transformation and multi-soliton solutions to the KdV equation with general variable coefficients*, Physics Letters A 287 (3-4) (2001) 211–216.
- [26] K. J. Wang, J. H. Liu, *Periodic solution of the time-space fractional Sasa-Satsuma equation in the monomode optical fibers by the energy balance theory*, Europhysics Letters 138 (2) (2022) 25002.